Desalination and Water Treatment
www.deswater.com

doi: 10.1080/19443994.2015.1060171

57 (2016) 13733–13746
June

Taylor & Francis
Taylor & Francis Group

Removal of heavy metal ions from aqueous solution by superabsorbent poly (NIPAAm/DAPB/AA) amphoteric nanohydrogel

Viran P. Mahida, Manish P. Patel*

Department of Chemistry, Sardar Patel University, Vallabh Vidyanagar, Gujarat 388120, India, Tel. +91 02692 226856; emails: viranmahida@gmail.com (V.P. Mahida), patelmanish1069@yahoo.com (M.P. Patel)

Received 19 January 2015; Accepted 3 June 2015

ABSTRACT

The present study demonstrates the synthesis of superabsorbent poly (NIPAAm/DAPB/AA) amphoteric nanohydrogels by inverse microemulsion polymerization and its application for the removal of heavy metal ions such as Pb(II) and Hg(II) from aqueous solution. Difference between with and without metal ions-adsorbed nanohydrogels was characterized by FT-IR, TGA, SEM, and EDX analyses. The particle size distribution of hydrogel nanoparticles was predicted by TEM micrograph to be between 30 and 40 nm. Specific surface area and pore volume of nanohydrogel were investigated with BET and BJH analysis. Maximum removal efficiency of Pb(II) and Hg(II) metal ions was investigated with treatment time, initial metal ion concentrations, pH values, and adsorbent dose. Finally, the equilibrium removal efficiency was analyzed according to the Langmuir and Freundlich adsorption isotherm model. From the adsorption studies, the maximum removal efficiency of metal ions toward the nanohydrogel was found to be in the following order: Pb(II) > Hg(II).

Keywords: Removal; Heavy metal ions; Superabsorbent; Nanohydrogel; Microemulsion polymerization

1. Introduction

Nowadays, the natural water bodies receive a large volume of wastewater containing heavy metals as a result of the increase in industrial activities [1,2]. According to the World Health Organization (WHO), the most important heavy metals of concern includes lead, cadmium, zinc, nickel, cobalt, chromium, copper, and mercury. Contamination of serviceable water by such heavy metal ions causes a severe public health problem, and it can also be toxic to aquatic life. Lead metal ions are potentially toxic for humans via interaction with sulfhydryl group of proteins. Also, it can be toxic to aquatic lives by causing reduction in root growth and loss of apical dominance of plants [3,4]. In addition, adverse health effect due to mercury has been reported to cause peripheral neuropathy, skin discoloration, swelling, and desquamation [5]. Due to the aspect behind this, it is very important to remove such heavy metal ions from natural environments.

Recently, adsorption is the most promising process due to its high efficiency, ease of operation, and cost-effectiveness [6,7]. In this respect, researchers are interested to work with superabsorbent hydrogels as the selective adsorbent material for the removal of such heavy metal ions from wastewater [8–10]. Superabsorbent hydrogels have been prepared with different functional monomers having hydroxyl,

*Corresponding author.

amine, carboxylic acid, and sulfonic acid groups of hydrophilic polymers, which may be cross-linked by chemical or physical interactions. Such hydrophilic polymers, which can absorb, swell, and retain aqueous solutions up to hundred times to their own weight, are able to expand in volume with respect to changes in external parameters, such as pH, temperature, and ionic strength [11]. Also, hydrogels can control the diffusion process and bind chemical species through their polar functional groups. These functional groups existing in cross-linked polymeric materials can be manipulated easily for specific applications, such as functioning as complex agents for heavy metal ions removal from wastewater [12,13].

Therefore, superabsorbent hydrogels can be considered as a novel, highly responsive, and high-capacity adsorbent material for the removal of heavy metal ions. The adsorption process with strong affinity and high loading capacity for targeted metal ions has attracted much attention which led to the modification of superabsorbent [14]. In the last few years, modification in the properties of superabsorbent hydrogels to micro- or nanoscale was made by the incorporation of inorganic nanomaterials [15]. In recent times, researchers were mainly focused on the improvement of the swelling ability, gel strength, and mechanical and thermal stability of superabsorbent hydrogels [16,17]. Due to this reason, adsorption of heavy metal ions by superabsorbent hydrogels is very important for the selection of suitable adsorbent material to remove heavy metals from aqueous solution.

In this study, a series of superabsorbent poly (NIPAAm/DAPB/AA) amphoteric nanohydrogels have been synthesized by inverse microemulsion polymerization. The chemical structure of nanohydrogel was characterized by FT-IR, DSC, TGA, BET and BJH, SEM, and TEM analyses. In addition, removal efficiency of nanohydrogel toward Pb(II) and Hg(II) metal ions by different experimental conditions was investigated in aqueous solution. Finally, the equilibrium removal performance of the metal ions-adsorbed superabsorbent nanohydrogel was analyzed according to the Langmuir and Freundlich adsorption isotherm model.

2. Materials and methods

2.1. Materials

DAPB cationic monomer was synthesized in our laboratory and characterized by previously reported method [18]. *N*-isopropylacrylamide (NIPAAm) (Aldrich, 97%) was used as received and need not to be purified further. Acrylic acid (AA) (Himedia, 99%) was used as received. The surface-active radical initiator 2, 2′-azobisisobutyronitrile (AIBN) (Himedia, 98%) was recrystallized twice from methanol prior to use. Aerosol AOT ((2-hydroxyethyl sulfosuccinate) sodium salt) (Aldrich) as an anionic surfactant and the cross-linking agent and ethylene glycol dimethacrylate (EGDMA) (Aldrich, 98%) were used without further purification. The metal salts used in the adsorption studies were $Pb(NO3)_2$ (Samir Tech. Chem. Pvt. Ltd., >99%) and $HgCl_2$ (Himedia, >99%). Extra-pure-grade toluene (Merck, >99%) and analytical-grade ethanol, acetone, and diethyl ether were used as received. Double-distilled water was used throughout the experiments.

2.2. Instruments

Spectrophotometric analyses were carried out with Shimadzu 160-A UVvisible spectrophotometer. FT-IR spectra of with and without metal ions-adsorbed nanohydrogel were directly analyzed by a Perkin–Elmer GX-FTIR spectrophotometer using KBr pellets. The cloud point or LCST was determined by differential scanning calorimeter (DSC) with Perkin–Elmer Pyris-1 instrument. Thermal behaviors of with and without metal ions-adsorbed nanohydrogel were investigated with Perkin–Elmer Pyris-1 Thermo Gravimetric Analyzer (TGA). TEM photographs of hydrogel nanoparticles were taken using Philips Tecnai-20 transmission electron microscope. SEM images, EDX spectra, and % of metal ions adsorbed were taken through Nova Nano SEM 450. BET and BJH analysis for specific surface area and pore volume was performed using Nova 1000e. The pH of solutions was adjusted with very small amounts of 0.01 M hydrochloric acid and sodium hydroxide and determined using Eco Tester pH 1 instrument.

2.3. Synthesis of poly (NIPAAm/DAPB/AA) superabsorbent nanohydrogels

In this study, inverse microemulsion polymerization was employed to synthesize the poly (NIPAAm/DAPB/AA) superabsorbent nanohydrogels. The cationic DAPB monomer is adjusted for the ratio of hydrophilic and hydrophobic segment of the nanohydrogel, which produces the amphoteric nature of nanohydrogel framework for better adsorption. In a continuous phase, 0.5 g of AOT was added to 5 mL of toluene and stirred in dry N_2 for 30 min. The temperature of the flask was maintained at 60˚C using a temperature controller.

The disperse phase was prepared by dissolving the required amount of NIPAAm with different amounts

of DAPB and AA. The solution was stirred under N_2 till a homogeneous solution was obtained. The disperse phase was then added dropwise into continuous phase to form W/O microemulsion. A cross-linking agent, EGDMA, was added, followed by the addition of AIBN as a surface-active initiator. Total conversion was obtained after 7 h of reaction.

Formed hydrogels were then transferred to a 1-L beaker containing double-distilled water and left for 2–3 d by changing water at every 4 h of interval in order to remove the unreacted monomers and other reactants. The swollen gel was dried using acetone in order to confirm the porosity in hydrogel generated during solvent drying. The process was repeated till the dry hydrogel was obtained. Finally, the hydrogel was kept in vacuum oven to constant weight. The feed compositions and relative percentage swelling of the nanohydrogels (V-01–V-07) are given in Table 1.

2.4. Swelling behaviors of nanohydrogels

Swelling behaviors of poly (NIPAAm/DAPB/AA) superabsorbent nanohydrogels were determined by gravimetric method at 25°C by adopting a tea-bag [19].

Percentage swelling of nanohydrogels in double-distilled water and metal ions solution with respect to time is shown in Fig. 1. For swelling study, nanohydrogels were immersed in distilled water and in metal solutions (200 ppm each) up to 16 h until hydrogel mass ceased to change [20].

It is well known that water diffusion into the hydrogel network gives more swelling in water, while metal ions bonding with the functional groups of hydrogel decrease the ionic pressure of hydrogel, which is responsible for lower swelling in metal ions solution. From Fig. 1, it can be observed that percentage swelling of nanohydrogels increases with respect to time and attains a constant value after certain point.

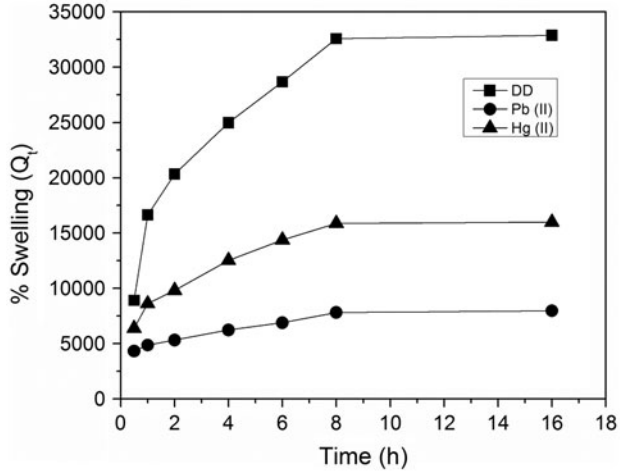

Fig. 1. Percentage swelling of nanohydrogel in double-distilled water and in metal ions solution with respect to time.

Nanohydrogels show maximum swelling in double-distilled water while minimum in Pb(II) metal ions solution. At the end of the swelling studies, it was observed that Pb(II) metal ions-adsorbed nanohydrogels showed lower swelling due to more binding capacity of nanohydrogels. The percentage swelling of nanohydrogels in distilled water and in metal ions solution is in the following order: Water > Hg(II) > Pb(II).

3. Results and discussion

Poly (NIPAAm/DAPB/AA) superabsorbent nanohydrogels with different monomeric ratios (V-01 to V-07) were synthesized by inverse microemulsion polymerization. Schematic representation of the synthesis of nanohydrogels is shown in Scheme 1. Sample-coded nanohydrogel V-03 shows high equilibrium percentage swelling after 8 h and stable and fast responsive

Table 1
The feed compositions and relative percentage swelling of the nanohydrogels (V-01–V-07)

Sr. no.	Sample code	NIPAAm	DAPB	AA	EGDMA	AIBN	(%) Swelling after 4 h	(%) Swelling after 8 h	(%) Swelling after 16 h
1	V-01	40	30	30	1	3	21,650	24,680	24,800
2	V-02	40	20	40	1	3	23,570	28,560	28,610
3	V-03	*40*	*10*	*50*	*1*	*3*	*24,980*	*32,580*	*32,880*
4	V-04	30	10	60	1	3	23,890	29,350	29,650
5	V-05	45	5	50	1	3	22,670	30,650	31,000
6	V-06	50	10	40	1	3	21,200	28,540	29,010
7	V-07	60	10	30	1	3	21,050	26,340	27,200

Note: The sample-coded (V-03) nanohydrogel (italic) shows the higher percentage swelling than the other synthesized nanohydrogels. So, this hydrogel feed composition is taken as the optimum reaction condition.

properties compared to other synthesized nanohydrogels; therefore, V-03 was utilized for further characterization and metal ions adsorption studies.

3.1. Characterization

3.1.1. FT-IR analysis

The FT-IR spectra of with and without metal ions-absorbed nanohydrogels are given in Fig. 2. FT-IR spectra explain the interaction between metal ions and functional groups of nanohydrogels, in which some bands were disappeared and shifting in certain peaks was observed [21]. The characteristic peak of N–H bond at 2,975 cm^{-1} was shifted to some lower frequency in both the metal ions-adsorbed nanohydrogels, indicating the participation of the –NH groups in adsorption. The quaternary amine is observed at 928 cm^{-1}, but it did not participate in the adsorption of metal ions. The characteristic peaks for –C=O groups were shifted to lower absorption in both the metal ions, which reveals the major participation of –C=O groups of ester and acid of nanohydrogels. It was also observed that the –C=O groups of *N*-isopropylacrylamide shifted to some lower frequency in both the metal ions-adsorbed nanohydrogels, indicating the contribution of –C=O groups in the metal ions adsorption.

3.1.2. DSC analysis

In order to investigate the lower critical solution temperature (LCST) of the nanohydrogel, DSC technique was employed. Fig. 3 shows the DSC curve of the synthesized nanohydrogel. From the figure, it is observed that nanohydrogel presented a broad peak located at around 82˚C due to higher content of AA (V-03). More hydrophilic moiety of AA in nanohydrogels will favor hydrogen bonding in preference to hydrophobic interactions and will increase the LCST of the copolymer. More hydrogen bonding requires additional energy to destroy it and results in the increase in LCST. Thus, LCST of nanohydrogels could be adjusted by changing the ratio of hydrophilic monomers in feed composition [22].

3.1.3. TGA analysis

The relative thermal stabilities of nanohydrogels were assessed by comparing the weight loss (%) vs. temperature range in between 50 and 700˚C. Overlay thermograms of V-03, Pb(II), and Hg(II) metal ions-adsorbed nanohydrogel are shown in Fig. 4. The thermal decomposition behavior of a polymer–metal complex depends on the macromolecular characteristics of the polymer base and the type of coordination

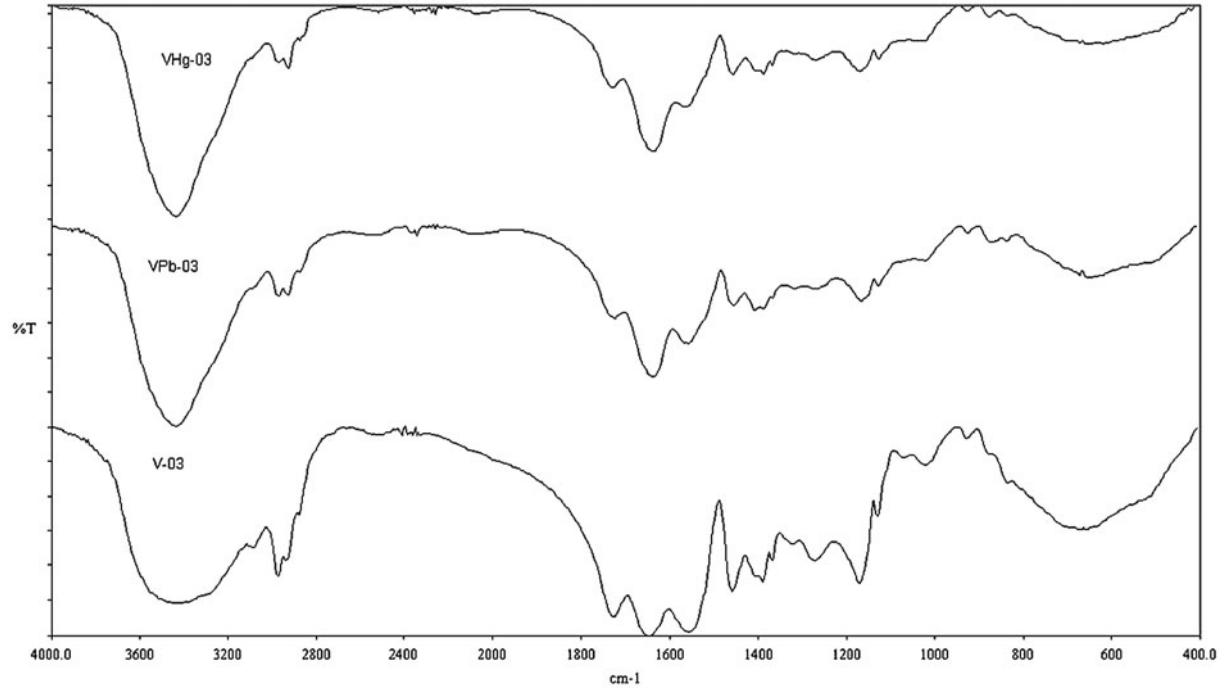

Fig. 2. FT-IR spectra of with and without metal ions-absorbed nanohydrogel.

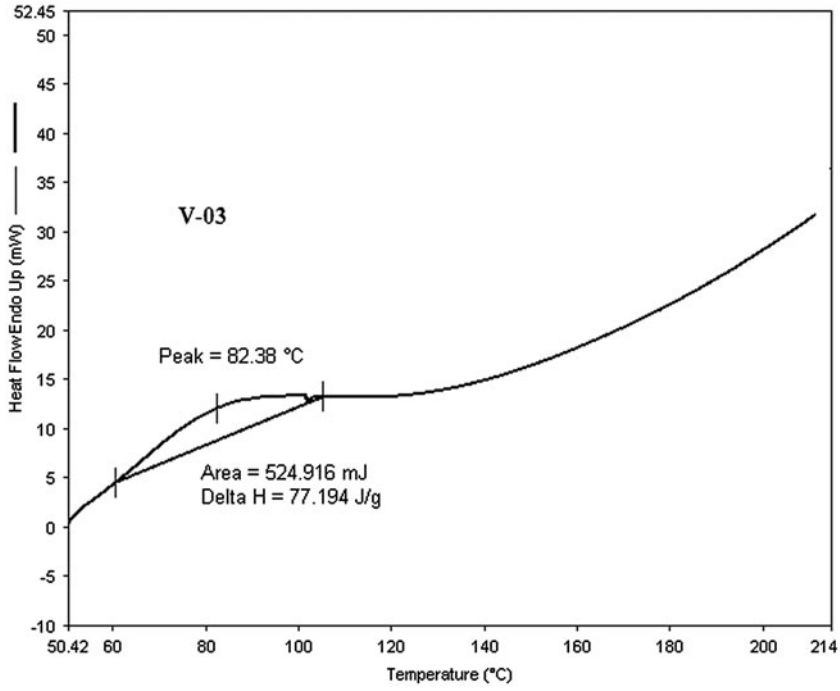

Fig. 3. DSC curve of the synthesized nanohydrogel.

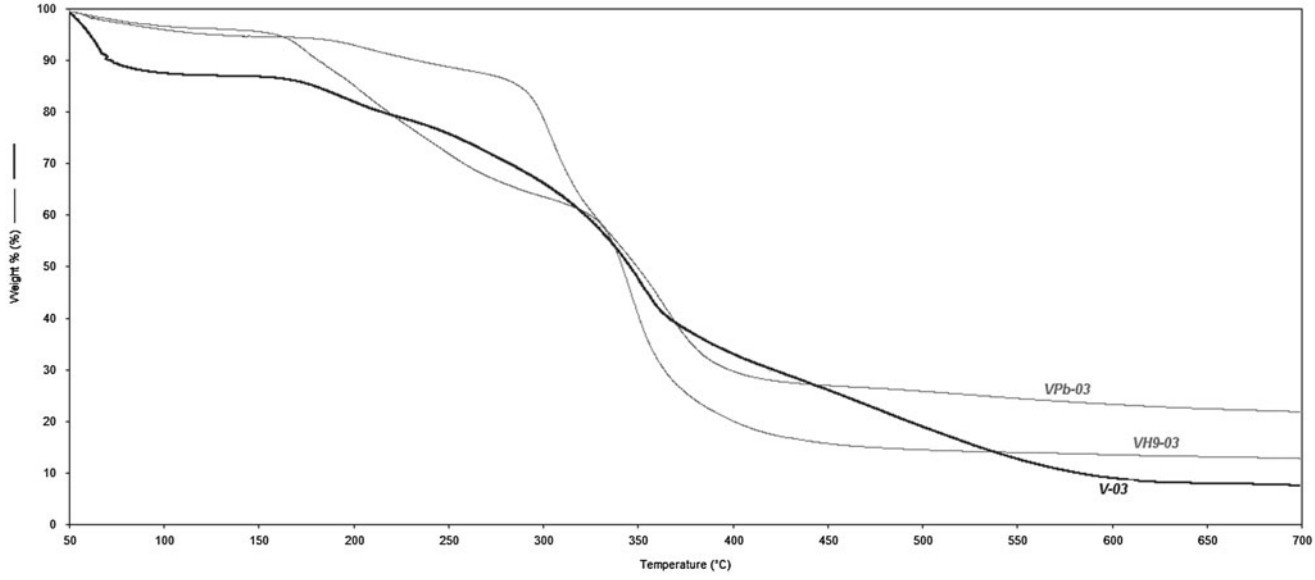

Fig. 4. Overlay thermograms of with and without metal ions-adsorbed nanohydrogel.

geometry. It is well known that for hydrogel, the high thermal stability of compounds indicates the stronger bonding due to the large adsorption of metal ions on its surface. Thermal stability depends on the bonding of molecule and/or types of bonds that occur between functional groups of nanohydrogel to metal ions [23]. The strongest bond, which requires more energy to break the bond, shows higher stability than the weak bond.

In this case, the interactions are mainly electrostatic, which arise between negative charge of polymer chain and the cationic charges of metal ions. Also, the

bonds between carboxylate ($–COO^-$) anions and Pb(II) and Hg(II) metal ions are ionic bonds, which require more energy to destroy it. Therefore, Pb(II) and Hg(II) metal ions-adsorbed nanohydrogels show high thermal stability than V-03 nanohydrogel. In the first degradation step, the loss of water molecules of V-03 nanohydrogel through the formation of intra-molecular and inter-molecular linkages takes place, which occurs more quickly (80–100˚C) than that of metal ions-adsorbed nanohydrogel. From the figure, it was also observed that Pb(II) metal ions-adsorbed nanohydrogels show more thermal stability than the Hg(II) metal ions-adsorbed nanohydrogels. Second degradation step, which shows the elimination of CO and CO_2 de-carboxylation of a fraction of the –COOH groups, occurs faster for V-03 nanohydrogels (200–250˚C) than the metal ions-adsorbed nanohydrogels (300–350˚C). Above 400˚C, relevant third degradation step, the decomposition of polymer starts, in which V-03 nanohydrogels decompose very fast, have lower stability, and give lowest chair value at 700˚C than Pb (II) and Hg(II) metal ions-adsorbed nanohydrogels.

3.1.4. TEM analysis

TEM micrograph of poly (NIPAAm/DAPB/AA) nanohydrogel is shown in Fig. 5. The particles were deposited onto the copper grid by deposition from a dilute suspension in acetone. The particle size distribution of the nanohydrogel was between 30 and 40 nm. From the micrograph, it was confirmed that the particles are almost spherical in shape. Smaller size of the particles was due to the high percentage of surface-active initiator and low percentage of crosslinker in the feed composition. Also, it fulfills the aim of the research that, by decreasing the particle size of hydrogels, which will increase the specific surface area, water as well as adsorption of dyes on its surface [24].

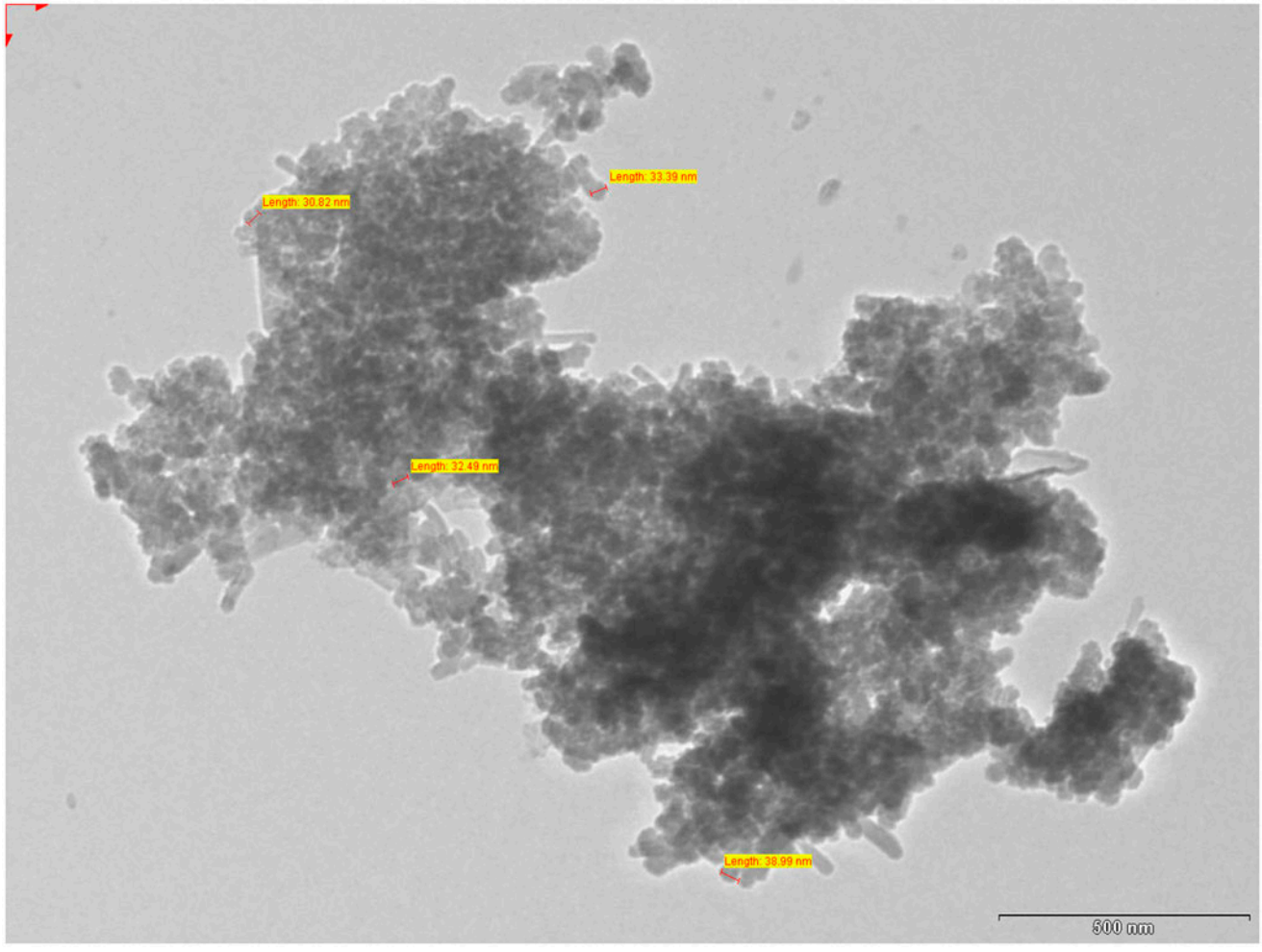

Fig. 5. TEM micrograph of nanohydrogel.

3.1.5. SEM analysis

The surface morphology of V-03 nanohydrogel and Pb(II) metal ions-adsorbed nanohydrogel was examined and is shown in Fig. 6. The figure explains the difference between before and after metal ions adsorption on V-03 nanohydrogel. In this case, the surface of nanohydrogel was changed due to high removal of Pb (II) metal ions. Before adsorption, the surface of V-03 nanohydrogel was uniform and porous due to solvent drying method, which filled up the metal ions adsorption [25].

3.1.6. BET and BJH analysis

Brunauer–Emmett–Teller (BET) and Barrett–Joyner–Halenda (BJH) analysis provides precise specific surface area and pore volume of nanohydrogel, respectively. Analysis was carried out by nitrogen multilayer adsorption and desorption technique measured as a function of relative pressure using a fully automated analyzer. Surface area and pore volume of nanohydrogel can play an important role for the dyes adsorption study [26]. It is well known that adsorption of water and metal ions increased as the surface area

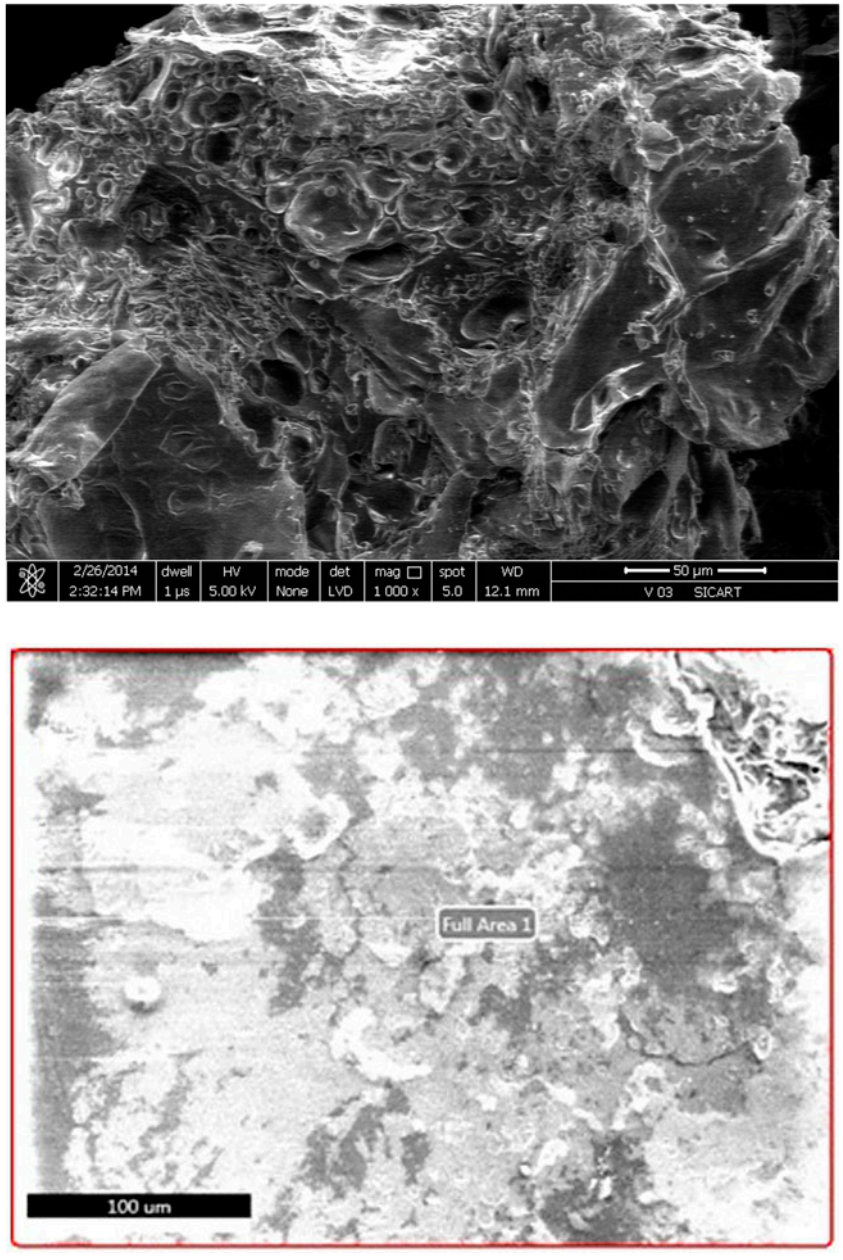

Fig. 6. Surf ace morphology of V-03 nanohydrogel and Pb(II) metal ions-adsorbed nanohydrogel.

Table 2
Specific surface area and pore volume of nanohydrogel (V-03)

BET Analysis of *specific surface area*	BJH Analysis of *pore volume*	
	BJH adsorption summary	BJH desorption summary
19.028 m^2/g	0.008 cc/g	0.008 cc/g

and pore volume of nanohydrogel increased. The detailed BET and BJH analysis of nanohydrogel is given in Table 2.

3.1.7. EDX analysis

It is well known that EDXA provides the qualitative elemental analysis localization on samples without destruction or injury to the samples [27]. The energy-dispersive X-ray (EDX) analysis distinguished the amount of Pb(II) and Hg(II) metal ions in nanohydrogel. Figures explain that high percentage (~14%) of Pb(II) metal ions was observed on the surface of the nanohydrogel compared to the Hg(II) metal ions (~6.74%). The detailed data of the EDXA are given in Table 3 and Fig. 7.

3.2. Removal study of Pb(II) and Hg(II) metal ions

It is well known that there are mainly two factors responsible for the interaction of metal ions and the adsorbent materials. First one is electrostatic interaction, which occurs between ionizable groups of nanohydrogel and specific charge of metal ions. While the other is hydrophobic interaction, in which hydrogen bond will be expected to occur between oxygen atoms (oxy anions) of metal ions with amine, methyl, and methine groups on the monomer unit of nanohydrogel. Plausible mechanism for the adsorption of metal ions toward nanohydrogel is shown in Scheme 2. In the present case, the interaction between metal ions and the nanohydrogel is mainly an electrostatic interaction. The negative charge of nanohydrogel chain formed a complex molecule with the positive charge of the cationic charge of metals, and it was also confirmed from FT-IR spectra and adsorption isotherms.

For the determination of different factors that affect the removal of metal ions such as treatment time, initial metal ions concentrations, pH, and adsorption dose, series of batch studies were conducted. Entire removal study and characterization were performed on nanohydrogel V-03 as it has maximum percentage swelling. Removal study was carried out by taking specified amount (0.025 g) of adsorbent in 50 mL of metal ions solution at various initial concentrations (100–500 ppm), pH values (pH range 2–14), and adsorption doses (10–50 mg). After equilibrium, concentration of metal ions remaining in the solution was determined with a UV–visible spectrophotometer after 8 h. Maximum adsorption capacity and/or % removal efficiency (RE %) of nanohydrogels were calculated using the following Eqs. (1) and (2), respectively.

$$q_e = (C_0 - C_e)V/m \quad (1)$$

$$\mathrm{RE}\,(\%) = (C_0 - C/C_0) \times 100 \quad (2)$$

where q_e (mg/g) is the adsorbed amount of dye per unit mass of nanohydrogel; C_0 and C_e are the initial dye concentration (mg/L) and equilibrium concentration (mg/L), respectively; C is the concentration of dye at time t; V is the volume of the solution; and m is the amount of the nanohydrogel used (g).

Table 3
Results of EDX analysis

	% Weight				
Pb(II)-adsorbed nanohydrogel	Carbon (C)	Oxygen (O)	Nitrogen (N)	Chlorine (Cl)	Lead (Pb)
	51	12	3	–	14
Hg(II)-adsorbed nanohydrogel	Carbon (C)	Oxygen (O)	Nitrogen (N)	Chlorine (Cl)	Mercury (Hg)
	42.09	34.19	16.44	0.54	6.74

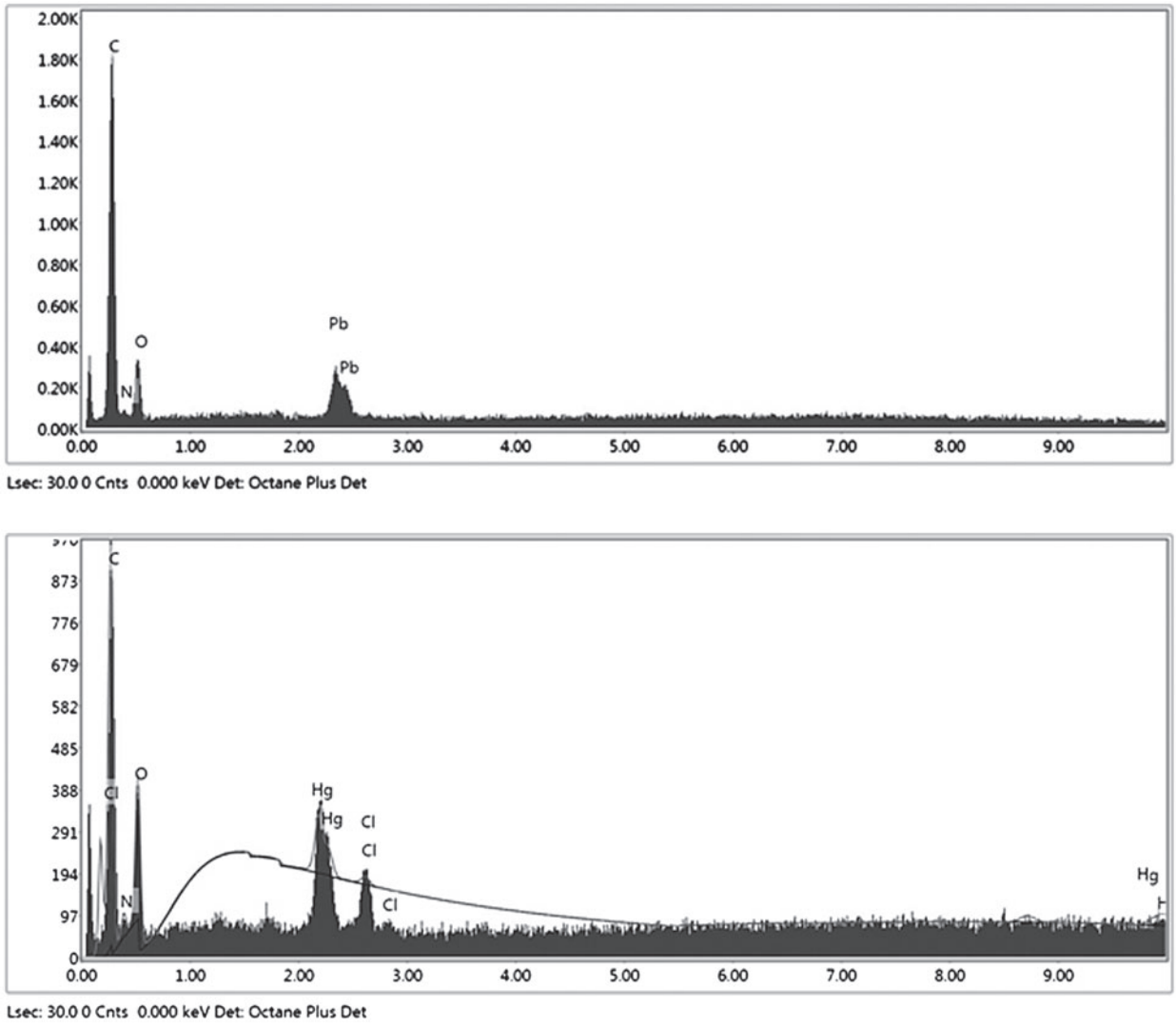

Fig. 7. EDX analysis of V-03 with (a) Pb(II) and (b) Hg(II)-adsorbed nanohydrogel.

3.2.1. Effect of treatment time

The effect of treatment time for Pb(II) and Hg(II) metal ions adsorption on the nanohydrogel V-03 is shown in Fig. 8. The maximum adsorption occurred in the first 2 h, then slows down, and finally achieved almost constant value after 8 h. No extreme change was observed when the treatment time was increased up to 16 h. The variation in treatment time showed that maximum removal efficiency of Pb(II) and Hg(II) metal ions was ~78 and ~63%, respectively. As expected, these results are in parallel with the results of the equilibrium percentage swelling of nanohydrogel [28].

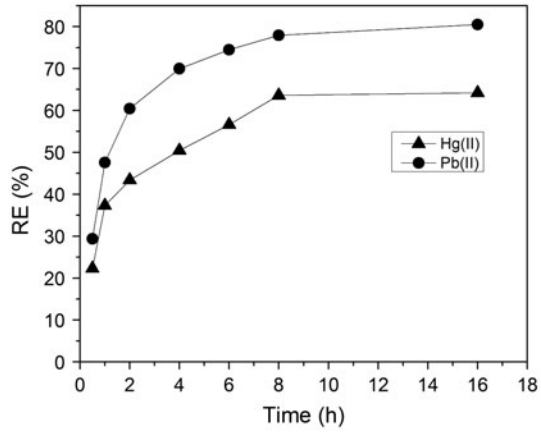

Fig. 8. The effect of treatment time for Pb(II) and Hg(II) metal ions adsorption.

3.2.2. Effect of initial metal ions concentration

For the determination of the effect of initial metal ions concentration on the adsorption, the nanohydrogel

was treated with a series of metal ions solution of gradually increasing concentrations [29]. Removal efficiency of the nanohydrogel with different initial metal ions solution concentrations is shown in Fig. 9. At lower metal ions solution concentrations, the removal efficiency of nanohydrogel is high, and thereafter, it slowly decreases due to the saturation of all the activated sites. The maximum removal efficiency of nanohydrogel toward Pb(II) and Hg(II) metal ions in 500 ppm solutions was ~72 and ~62%, respectively.

3.2.3. Effect of pH

The effect of pH on RE (%) of nanohydrogel is shown in Fig. 10. At lower pH values (2–4), the adsorption was negligible due to the protonated forms of carboxylic acid groups that are much less capable of forming complexes than salt forms. When metal ions solution has pH value of 6 or greater than 6, carboxylic groups ionized and dominated the maximum removal efficiency till pH value of the solution was 10. At higher pH value, the removal efficiency was decreased due to the formation of metal hydroxide from the free metal ion, which is usually less soluble and did not take part in the further metal ions adsorption [30].

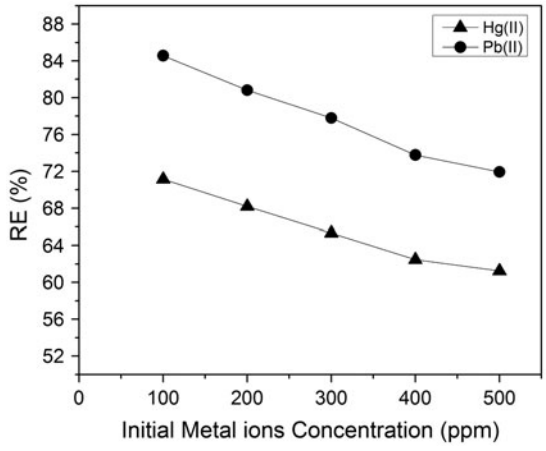

Fig. 9. Removal efficiency of the nanohydrogel with different initial metal ions solution concentrations.

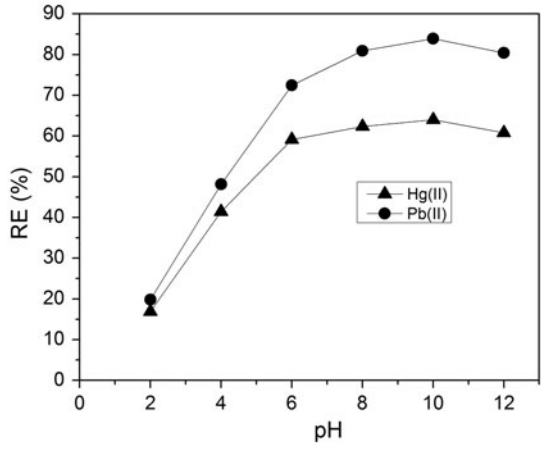

Fig. 10. The effect of pH on RE (%) of nanohydrogel.

3.2.4. Effect of adsorption dose

Removal efficiency of nanohydrogel toward Pb(II) and Hg(II) metal ions at different contents of adsorbent is shown in Fig. 11. This figure shows that, by increasing the adsorbent content, the removal efficiency of nanohydrogel increased. After maximum adsorption, increasing the adsorbent content had negligible effect on the removal of metal ions. These happen as all active sites were filled with the maximum metal ions, and hence, no active sites are available for the adsorption of metal ions.

3.3. Desorption and reusability studies

Various eluents were used for the desorption study of Pb(II) and Hg(II) metal ions-adsorbed nanohydrogel. In this case, 0.1 M HNO_3 was used for desorption of both the metal ions from the nanohydrogel. The adsorption process was carried out for Pb(II) and Hg (II) metal ions at 100-ppm solution. The metal ions-adsorbed nanohydrogel (0.025 g) was treated appropriately with 0.1 M HNO_3 solution and stirred for 2 h at 300 rpm. The process was repeated until the maximum

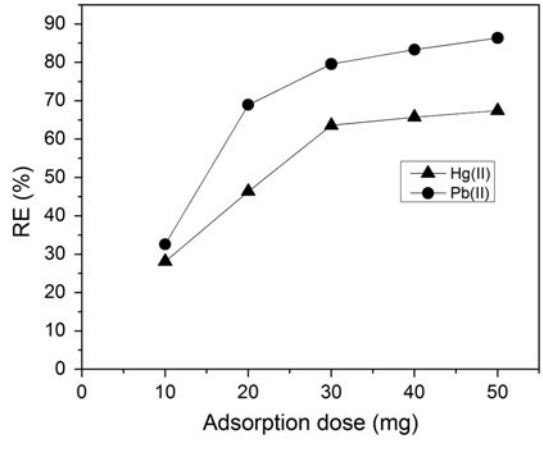

Fig. 11. Removal efficiency of Pb(II) and Hg(II) metal ions at different contents of adsorbent.

desorption of metal ions was achieved. After the desorption study, the uptake percentage of nanohydrogel decreased from 84.57 to 18.41% for Pb(II) metal ions and from 71. 15 to 12.53% for Hg(II) metal ions. The nanohydrogel was able to adsorb metal ions for two cycles, and after that, very low adsorption was observed. Also, weight loss occurred during each run in the metal ions desorption study [31].

3.4. Adsorption isotherm models

The analysis and design of the adsorption process requires the relevant adsorption isotherms. Adsorption equilibrium provides fundamental physicochemical data for evaluating the applicability of the process as a unit operation. The data obtained were analyzed using the Langmuir and Freundlich isotherms [32]. The linear form of the Langmuir and Freundlich isotherms is described by Eqs. (3) and (4), respectively.

$$1/q_e = 1/q_0 + 1/q_0 b C_e \quad (3)$$

$$\log q_e = \log K_f + 1/n \log C_e \quad (4)$$

where q_e is the amount of metal ions adsorbed (mg/g) toward nanohydrogel, q_0 is the maximum adsorption capacity related to Langmuir adsorption (mg/g), and C_e is the residual concentration of metal ions at equilibrium (mg/L). K_f and n are the Freundlich constants that predict the amount of metal ions adsorbed per gram of adsorbent at equilibrium concentration and strength of the adsorption process, respectively. Detailed explanation is given in Figs. 12 and 13, and the Langmuir and Freundlich isotherms parameters are given in Table 4.

From Table 4, it is clear that value of R^2 for both the Pb(II) and Hg(II) metal ions of linear form of the Langmuir model and the Freundlich model is almost equal to unit number. This indicates that the adsorption of Pb(II) and Hg(II) metal ions on the nanohydrogel fitted not only the Langmuir isotherm model, but also the Freundlich model. From the Langmuir isotherm, it is clear that the maximum adsorption capacities (q_0) for Pb(II) and Hg(II) metal ions on nanohydrogel were 1,250 and 1,111.11 (mg/g), respectively. Also, it is well known that for Freundlich isotherms, the parameter $n > 1$ indicates favorable adsorption. For both the metal ions-adsorbed nanohydrogels, all the calculated n values of Freundlich

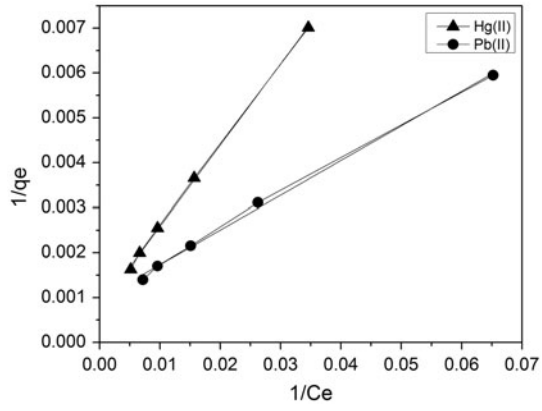

Fig. 12. Langmuir isotherm for the adsorption of metal ions.

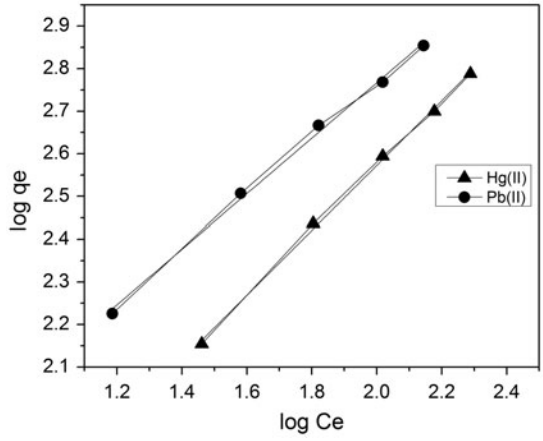

Fig. 13. Freundlich isotherm for the adsorption of metal ions.

Table 4
Langmuir and Freundlich isotherm parameters for the adsorption of metal ions on nanohydrogel (V-03)

		Langmuir isotherm			*Freundlich isotherm*		
Sr. no.	Metal ions	R^2	q_o	B	R^2	K_f	n
1	Pb(II)	0.9993	1,250	0.0044	0.9962	0.3819	1.5361
2	Hg(II)	0.9968	1,111.11	0.0116	0.998	0.0152	1.3156

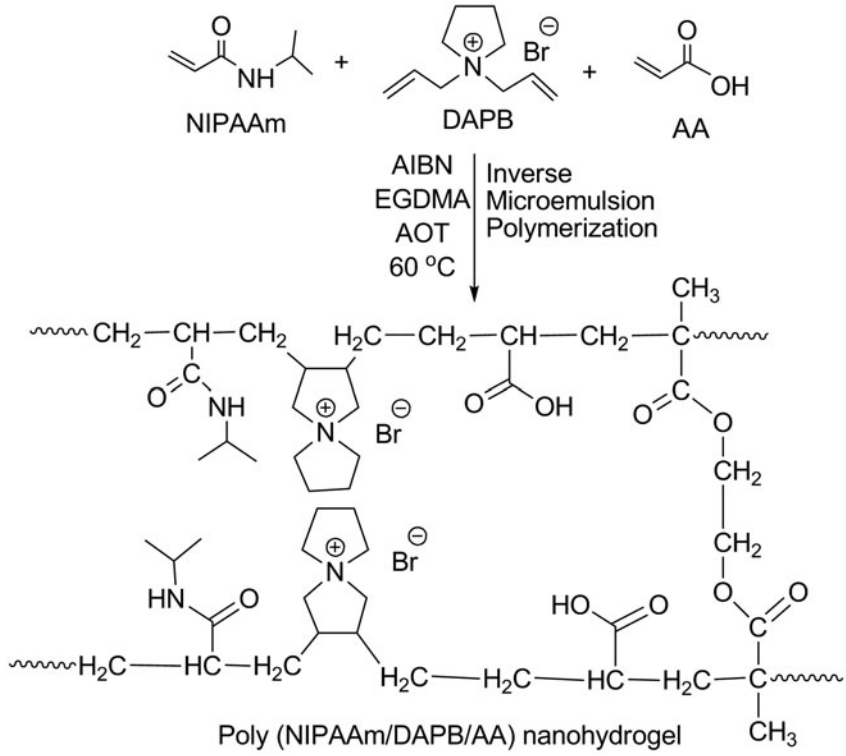

Scheme 1. Reaction scheme of poly (NIPAAm/DAPB/AA) nanohydrogel.

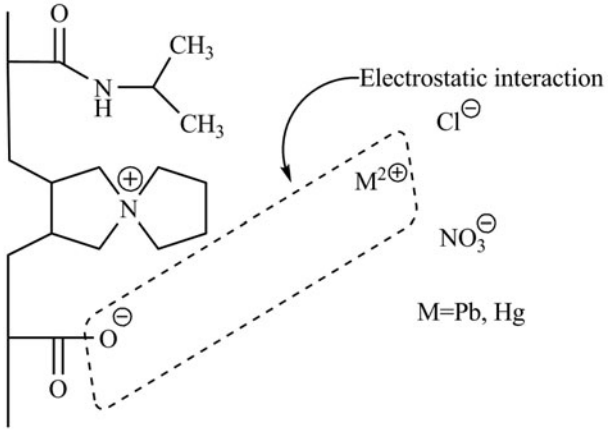

Scheme 2. Plausible mechanism for the adsorption of metal ions towards nanohydrogel.

isotherm are in the range of 1–3 indicating that the adsorption intensity was favorable at high concentration but much less at lower concentration. From the detailed study, it can be easily concluded that we were getting maximum adsorption and high removal efficiency of Pb(II) and Hg(II) metal ions toward the synthesized nanohydrogel.

4. Conclusion

This investigation deals with the synthesis of superabsorbent poly (NIPAAm/DAPB/AA) nanohydrogels by inverse microemulsion polymerization and its application for the removal of heavy metal ions, such as Pb(II) and Hg(II), from aqueous solution. From the swelling studies, it was observed that lower percentage swelling of nanohydrogel in Pb(II) metal ions solution than Hg(II) metal ion and double-distilled water indicates the high adsorption of Pb(II) metal ions on V-03 nanohydrogel. FT-IR spectra explain that the polymeric chain possesses the negatively charged $-COO^-$ functionality, which is likely the main adsorption site for cationic Pb(II) and Hg(II) metal ions. After analyzing the TGA thermograms and EDX of both the metal ions-adsorbed nanohydrogels, the high adsorption of Pb(II) metal ions on nanohydrogel surface compared to Hg(II) metal ions was confirmed. Synthesized nanohydrogel had good adsorption capacity toward Pb(II) and Hg(II) metal ions and showed strong adsorption and high removal efficiency as the pH of metal ions solutions was increased up to pH 10; afterward, it decreased at a certain level. From the adsorption studies, it was concluded that the maximum removal efficiency of the

nanohydrogel toward Pb(II) and Hg(II) metal ions was ~84 and ~64%, respectively. The sorption data were analyzed according to Langmuir and Freundlich isotherm model, and it was observed that both the isotherm models may well obey the experimental data and have monolayer adsorption and purely electrostatic interaction. As per the adsorption studies, it is concluded that feasible improvements in the adsorption behaviors of nanohydrogel encourage its utility in wastewater treatment.

Acknowledgments

The authors gratefully acknowledge the Head of the Department of Chemistry at Sardar Patel University for research facilities. The authors also express their appreciation for the studies in the Sophisticated Instrument Center for Applied Research and Testing [SICART], Vallabh Vidyanagar, for FT-IR, DSC, TGA, SEM, TEM, and EDX analyses. Also, the authors gratefully acknowledge Heubach Colour Pvt. Ltd, Ankleshwar, for free-of-charge BET and BJH analysis. Financial support for this work was provided by the University Grant Commission, New Delhi, (Project Number: F.39-685/2010(SR)), to whom researches are gratefully acknowledged.

Abbrevations

NIPAAm	—	*N*-isopropylacrylamide
DAPB	—	*N*,*N*-diallylpyrrolidinium bromide
AA	—	acrylic acid
EGDMA	—	ethylene glycol dimethacrylate
AIBN	—	2,2´-azobisisobutyronitrile
AOT	—	aerosol ((2-hydroxyethyl sulfosuccinate) sodium salt)
Pb(II)	—	lead(II)
Hg(II)	—	mercury(II)

References

[1] V.K. Gupta, P. Singh, N. Rahman, Adsorption behavior of Hg(II), Pb(II), and Cd(II) from aqueous solution on Duolite C-433: A synthetic resin, J. Colloid. Interface. Sci. 275 (2004) 398–402.
[2] N. Prakash, P.N. Sudha, N.G. Renganathan, Copper and cadmium removal from synthetic industrial wastewater using chitosan and nylon 6, Environ. Sci. Pollut. Res. 19 (2012) 2930–2941.
[3] M. Firlak, E.K. Yetimoglu, M.V. Kahraman, N.K. Apohan, S. Deniz, Removal of lead and cadmium ions from aqueous solutions using sulphur and oxygen donor ligand bearing hydrogels, Sep. Sci. Technol. 45 (2010) 116–128.
[4] P.C. Mishra, M. Islam, R.K. Patel, Removal of lead(II) by chitosan from aqueous medium, Sep. Sci. Technol. 48 (2013) 1234–1242.
[5] T. Tripathy, H. Koyla, S. Das, Synthesis of Starch-g-Poly-(N-methylacrylamide-co-acrylic acid) and its application for the removal of mercury(II) from aqueous solution by adsorption, Eur. Polym. J. 58 (2014) 1–10.
[6] L. Zhong, X. Peng, L. Song, D. Yang, X. Cao, R. Sun, Adsorption of Cu^{2+} and Ni^{2+} from aqueous solution by arabinoxylan hydrogel: Equilibrium, kinetic, competitive adsorption, Sep. Sci. Technol. 48 (2013) 2659–2669.
[7] P.V. Dadhaniya, A.M. Patel, M.P. Patel, R.G. Patel, A new cationic poly[1-vinyl-3-ethyl imidazolium iodide], P(VEII) hydrogel for the effective removal of Chromium (VI) from aqueous solution, Pure Appl. Chem. J. Macromol. Sci., Part A 46 (2009) 447–454.
[8] S.S. Saber-Samandari, M. Gazi, Removal of mercury(II) from aqueous solution using chitosan-graft-polyacrylamide semi-IPN hydrogels, Sep. Sci. Technol. 48 (2013) 1382–1390.
[9] V.P. Mahida, M.P. Patel, Synthesis of new superabsorbent poly (NIPAAm/AA/*N* -allylisatin) nanohydrogel for effective removal of As(V) and Cd(II) toxic metal ions, Chin. Chem. Lett. 25 (2014) 601–604.
[10] S.K. Bajpai, S. Johnson, Removal of Ni^{2+} ions from aqueous solution by sorption into poly (Acrylamide-co-sodium acrylate) hydrogels, J. Macromol. Sci., Part A Pure Appl. Chem. 44 (2007) 285–290.
[11] V.P. Mahida, M.P. Patel, Removal of some most hazardous cationic dyes using novel poly (NIPAAm/AA/*N*-allyisatin) nanohydrogel Arab. J. Chem. (in press), doi: 10.1016/j.arabjc.2014.05.016.
[12] C.P. Mane, S.V. Mahamuni, A.P. Gaikwad, R.V. Shejwal, S.S. Kolekar, M.A. Anuse, Extraction and separation of mercury(II) from succinate media with high molecular weight amine as an extractant. J. Saudi. Chem. Soc. 19 (2015) 46–53, doi: 10.1016/j.jscs.2011.12.016.
[13] A.M. Patel, R.G. Patel, M.P. Patel, Nickel and copper removal study from aqueous solution using new cationic poly [acrylamide/N, N-DAMB/N, N-DAPB] super absorbent hydrogel J. Appl. Polym. Sci. 119 (2011) 2485–2493.
[14] I.L. Lagadic, M.K. Mitchell, B.D. Payne, Highly effective adsorption of heavy metal ions by a thiol-functionalized magnesium phyllosilicate clay, Environ. Sci. Technol. 35 (2001) 984–990.
[15] H. Kaşgöz, A. Durmuş, A. Kaşgöz, Enhanced swelling and adsorption properties of AAm-AMPSNa/clay hydrogel nanocomposites for heavy metal ion removal, Polym. Adv. Technol. 19 (2008) 213–220.
[16] M.S. Alhakawati, C.J. Banks, Removal of copper from aqueous solution by *Ascophyllum nodosum* immobilised in hydrophilic polyurethane foam, J. Environ. Manage. 72 (2004) 195–204.
[17] U. Ulusoy, S. Simsek, Lead removal by polyacrylamide-bentonite and zeolite composites: Effect of phytic acid immobilization, J. Hazard. Mater. 127 (2005) 163–171.
[18] Y.N. Patel, M.P. Patel, Novel cationic poly [AAm/NVP/DAPB] hydrogels for removal of some textile anionic dyes from aqueous solution, J. Macromol. Sci., Part A Pure Appl. Chem. 49 (2012) 490–501.

[19] Ömer Barış Üzüm, E. Karadağ, Swelling characterization of poly (acrylamide-co-N-vinylimidazole) hydrogels crosslinked by TMPTA and semi-IPN's with PEG, J. Polym. Res. 14 (2007) 483–488.
[20] P.V. Dadhaniya, M.P. Patel, R.G. Patel, Copper and nickel removal from aqueous solutions using new chelating poly [acrylamide/ N-vinyl pyrrolidone/3-(2-hydroxyethyl carbamoyl) acrylic acid] Hydrogels, J. Macromol. Sci., Part A Pure Appl. Chem. 44 (2007) 769–777.
[21] M. Fırlak, S. Çubuk, E.K. Yetimoğlu, M.V. Kahraman, Uptake of Pb^{2+} using n-vinyl imidazole based uniform porous hydrogels, Sep. Sci. Technol. 46 (2011) 1984–1993.
[22] L.G. Guerrero-Ramirez, S.M. Nuno-Donlucas, L.C. Cesteros, I. Katime, Novel functionalized nanohydrogels, synthesis and some applications, J. Phys. Conf. Ser. 127 (2008) 1–10.
[23] N. Nishat, A. Malik, Synthesis, spectral characterization thermal stability, antimicrobial studies and biodegradation of starch-thiourea based biodegradable polymeric ligand and its coordination complexes with [Mn(II), Co(II), Ni(II), Cu(II), and Zn(II)] metals, J. Saudi Chem. Soc. (in press), doi: 10.1016/j.jscs.2012.07.017.
[24] I. Mobasherpour, E. Salahi, M. Pazouki, Removal of nickel(II) from aqueous solutions by using nanocrystalline calcium hydroxyapatite, J. Saudi Chem. Soc. 15 (2011) 105–112.
[25] G.Z. Kyzas, N.A. Travlou, E.A. Deliyanni, The role of chitosan as nanofiller of graphite oxide for the removal of toxic mercury ions, Colloids surf., B: Biointerfaces 113 (2014) 467–476.
[26] A. Dawlet, D. Talip, H.Y. Mi, M. MaLiKeZhaTi, Removal of mercury from aqueous solution using sheep bone charcoal, Procedia Environ. Sci. 18 (2013) 800–808.
[27] R.A.K. Rao, M. Kashifuddin, Adsorption studies of Cd (II) on ball clay: Comparison with other natural clays. Arab. J. Chem. (in press), doi: 10.1016/j.arabjc.2012.01.010.
[28] B.L. Rivas, I.M. Perič, S. Villegas, Synthesis and metal ion uptake properties of water-insoluble functional copolymers: Removal of metal ions with environmental impact, Polym. Bull. 65 (2010) 917–928.
[29] M. Zendehdel, A. Barati, H. Alikhani, Removal of heavy metals from aqueous solution by poly(acrylamide-co-acrylic acid) modified with porous materials, Polym. Bull. 67 (2011) 343–360.
[30] A. Ali, H.A. Shawky, H.A. Rehim, E.A. Hegazy, Synthesis and characterization of PVP/AAc copolymer hydrogel and its applications in the removal of heavy metals from aqueous solution, Eur. Polym. J. 39 (2003) 2337–2344.
[31] J.P. Laurino, Removal of lead(II) ions by poly (2-octadecyl butanedioic acid): Isothermal and kinetic studies, J. Macromol. Sci. Part A Pure Appl. Chem. 45 (2008) 612–619.
[32] K. Kesenci, R. Say, A. Denizli, Removal of heavy metal ions from water by using poly(ethyleneglycol dimethacrylate-co-acrylamide) beads, Eur. Polym. J. 38 (2002) 1443–1448.